

6 OPTICS

6.1 Introduction

The GMT Project is developing a high-performance, compact ELT that capitalizes on the technology base that has been developed for a succession of current-generation large telescopes (MMT, Magellan, LBT). Those telescopes are designed around lightweight borosilicate primary mirrors that can be cast in diameters up to 8.4 meters at the University of Arizona Steward Observatory Mirror Lab (SOML). GMT will have a segmented primary mirror consisting of six 8.4 meter, off-axis, circular mirrors arranged in a hexagon and a seventh 8.4 meter mirror in the center as shown in Figure 6-1.

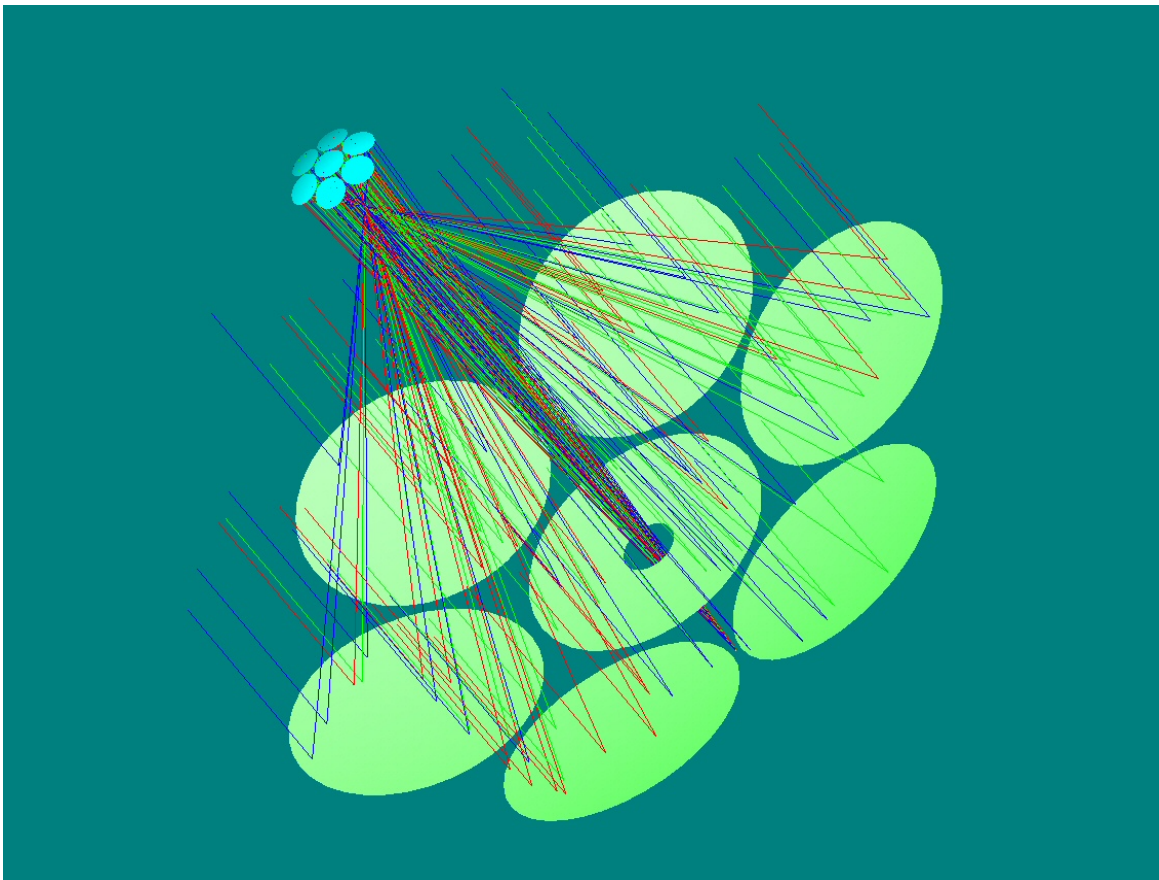


Figure 6-1. GMT segmented mirror optics illuminated with a random distribution of rays.

The technology developed for producing the segments allows a very fast ($f/0.7$) primary mirror focal ratio contributing to the overall compactness of the GMT structure and reducing the size of the $f/8.0$ secondary mirror, correctors, and instrumentation. The $f/8.0$ final focal ratio was chosen to optimize the beam size in the re-imaging spectrographs as described in Section 6.2.1. The production of primary mirror segments, flotation supports, and thermal control is described in Chapter 10.

The GMT optical design uses an aplanatic Gregorian prescription with a concave secondary mirror. The baseline adaptive secondary mirror is segmented with the segments conjugated to the primary mirror segments. The concave shape has a number of fabrication and performance advantages described in the next section. The front surface of the secondary mirror will be adaptive using the technology developed for the MMT 64 cm and LBT 90 cm AO secondary mirrors as described in Chapter 11. A non-adaptive, segmented, secondary mirror will be provided as a backup to the adaptive secondary mirror and for commissioning the telescope.

A corrector and atmospheric dispersion compensator (ADC) will be provided for wide-field, natural seeing, operation in the visible band. This will allow observations over a field of view up to 20 arcminutes (goal: 24 arcminutes). The corrector and ADC will be removable for work on smaller fields and in other wavelengths. Designs for the corrector/ADC are described in section 6.3.

The telescope will focus 5.50 meters below the primary mirror vertex (5.67 meters with the corrector and ADC). Large instruments and those requiring a direct view with minimum number of reflections (e.g. mid-IR instruments) will mount at this location. One or more deployable tertiary mirrors, some of them dichroic, will redirect the beam to small- to medium-size instruments located on a platform above the straight-through focus and will allow rapid switching between instruments. The plans for how the switching is accomplished and instrumentation are described in the Chapter 9, Adaptive Optics and Chapter 13, Scientific Instrumentation .

The optical prescription and performance of the GMT optical system is described in the following sections [6.2-6.5]. Alignment tolerances are discussed in Chapters 8. Fabrication tolerances for the primary mirror are discussed in Chapter 10 in relation to the image error budgets of Chapter 12.

6.2 Basic Aplanatic Gregorian Design

6.2.1 Prescription

The basic two-mirror design for the GMT without corrector is an aplanatic Gregorian configuration using segmented primary and secondary mirrors. The 18.0 meter primary mirror focal length and 25.4 meter full aperture give the primary mirror assembly an $f/0.7$ focal ratio. The effective focal length for the combined primary-secondary mirror system is 203 meters ($f/8.0$) with the focus located 5.5 meters below the primary mirror vertex.

The primary mirror segments form a common surface with the parent ellipsoidal design sharing a common optical axis passing through the center of the middle segment. The physical spacing between segments is 295 mm from one off-axis segment to another off-axis segment, and 359 mm from an off-axis segment to the center segment. The 1.78 m diameter hole in the center segment provides a 24 arcminute unvignetted field of view with corrector. It will likely be increased to around 1.9 m (26') during design development.

The secondary mirror segments are sized to match the zero-degree-field beam size of the primary mirror subapertures. The implications for the telescope emissivity in the thermal IR are discussed in Section 6.2.4. The telescope has an effective on-axis collecting area of 375.6 m², roughly the equivalent of a 21.9 m diameter circular mirror with the same central obscuration.

Table 6-1 gives the basic telescope optical prescription.

Table 6-1. GMT Optical Prescription (no corrector).

Primary Mirror (M1)		
Configuration	Segmented	Seven (7) x 8.4 m dia. Segments.
Diameter, D1	25.448 meters	Non-circular aperture.
Radius of curvature, R1	36.000 meters	
Conic constant, K1	-0.99829	
Segment diameter, D _{c1}	8.365 meters	Circular clear aperture. Off-axis segments tilted 13.522°.
Center hole diameter.	1.78 meters	
Secondary Mirror (M2)		
Configuration	7 segments	Conjugated with M1 segments.
Diameter, D2	3.2 meter	Pupil stop. Non-circular aperture.
Radius of curvature, R2	4.2058 meters	
Conic constant, K2	-0.71087	
Segment diameter, D _{c2}	1.063 meter	
Combined (M1,M2)		
M1-M2 separation, S	20.290 meters	
M1 to focal plane separation	5.500 meters	
Focal length, FL	202.745 meters	
Focal ratio, f	f/8.0	Full 25.4m clear aperture.
Effective area, A	368 m ²	With 3.2 meter circular M2 baffle.
Field curvature	2.203 meters	Towards instrument.

The Gregorian design was chosen for a number of reasons: (1) the secondary is optically conjugated to a position ~160 meters above the ground, enabling excellent ground layer adaptive optics correction over a large field of view, (2) the Gregorian design allows in-telescope calibration of the AO system with an artificial star at prime focus (not possible with a Cassegrain design), and (3) the curvature of the telescope focal plane is in the right direction, curved towards the instrument, to optimize the design of the collimator for a wide-field, multi-object, seeing-limited spectrograph (see Section 13.6). In addition, unlike in a Cassegrain configuration, a flat field screen may be deployed at the exit pupil of the telescope at a position below the secondary mirror with a direct line-of-sight to the instruments. The Gregorian penalty paid in a longer telescope structure is minimized by the fast primary focal ratio. Adopting an aplanatic

prescription (i.e. non-parabolic primary mirror) eliminates field coma in the off-axis images and gives a wider uncorrected field of view.

The current GMT optical design is the result of a series of design studies which were carried out prior to casting the first primary mirror segment. The design of the wide-field collimator drives the choice of the secondary focal ratio, but does not place a strong constraint on the focal length of the primary. In fact the primary mirror focal length was chosen to be as fast as possible considering the technical difficulty of testing the off-axis mirror segments. The secondary focal ratio was chosen to be consistent with a wide-field collimated beam diameter of 300 mm. In addition, the size of the wide-field secondary focal plane is consistent with practical limits on the sizes of optical glass blanks for the corrector/ADC.

6.2.2 Image Quality

The geometric spot sizes for the segmented mirror narrow-field configuration without the corrector and ADC are shown in Figure 6-2. The usable field of view without the wide-field corrector will be limited by off-axis field aberrations, principally astigmatism, in the two mirror aplanatic design.

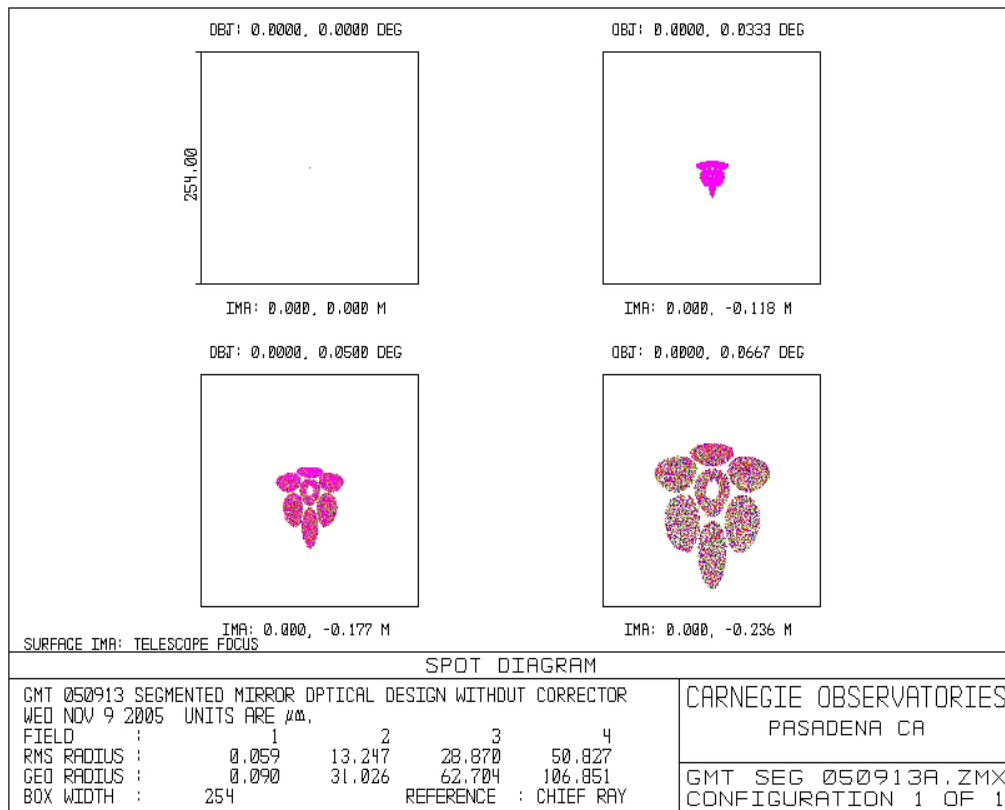


Figure 6-2. GMT geometric spot sizes for 0', 2', 3', and 4' field radii. The box size is 0.25".

6.2.3 Diffraction performance

The on-axis point spread at 500 nm is shown in Figure 6-3. The box size is 0.25 arcsecond².

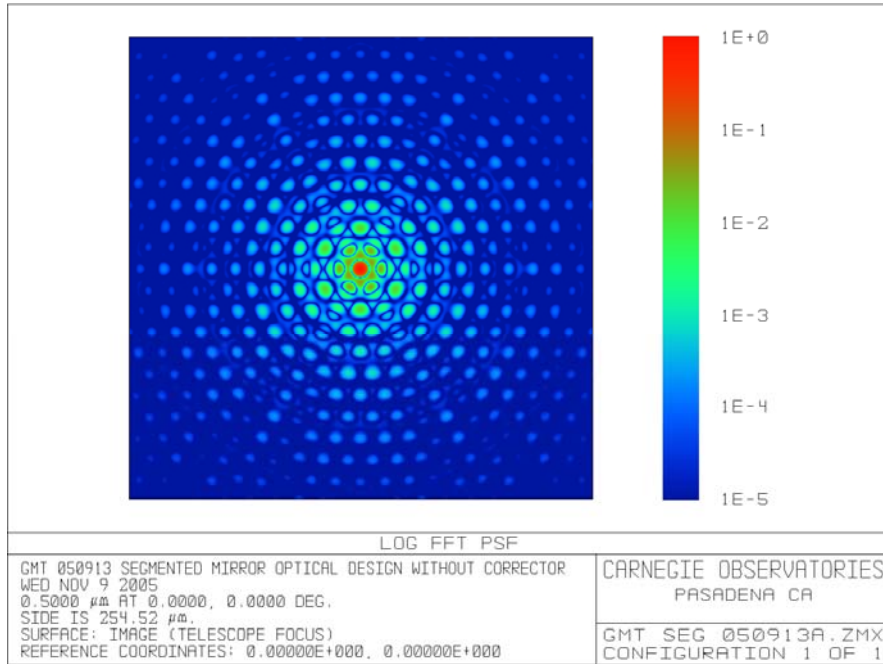


Figure 6-3. Center field point spread function at the reference wavelength of 500 nm (shown in a 0.25" box).

The enclosed energy for field radii 0', 2', 3', and 4' at 500 nm is shown in Figure 6-4 out to a radius of 0.125 arcsecond.

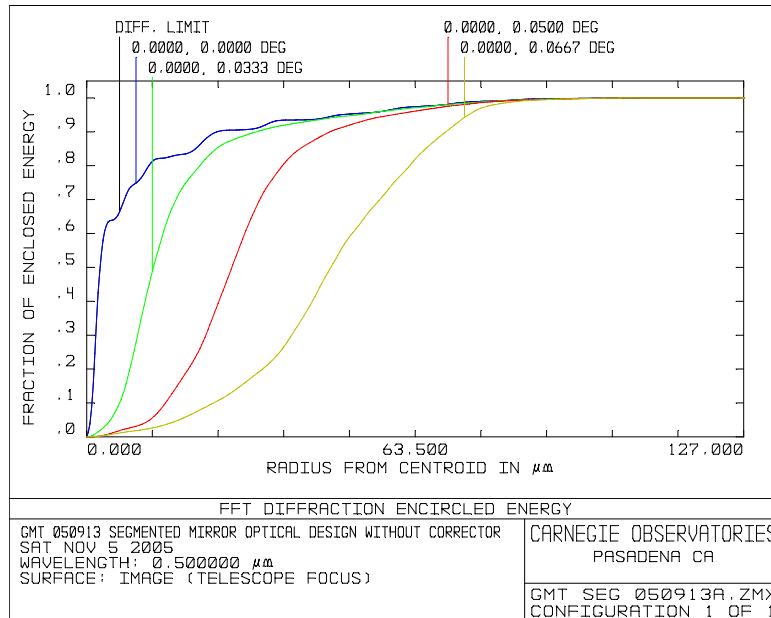


Figure 6-4. Enclosed energy plot for the narrow field GMT configuration at the reference wavelength 500 nm at field angles of 0', 2', 3' and 4'. The maximum radius shown is 0.125".

Figure 6-5 shows the GMT point spread function at 1.65 microns compared to a filled 24.5 meter aperture. GMT has comparable resolution although with 77% of the throughput.

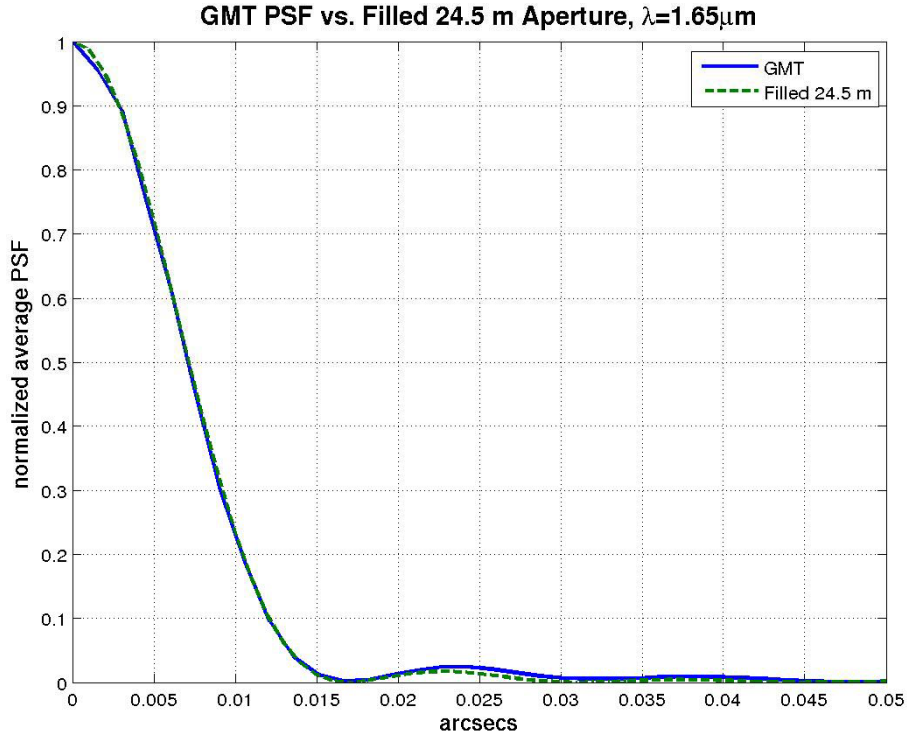


Figure 6-5. Point spread function of GMT at 1.65 microns compared to the PSF for a 24.5 meter filled aperture telescope.

6.2.4 Emissivity

The background radiation from telescope optics can be significant for wavelengths longer than $\sim 2 \mu\text{m}$ where the thermal emission of the optics is significant. The level of this background radiation is typically characterized in terms of a fraction of the equivalent blackbody radiation for the ambient temperature of the telescope. This is useful since the source of the background radiation is typically dominated by the emissivity (or 1 minus the reflectivity) of the reflecting surfaces. An additional contribution is radiation from the surrounding warm telescope structure. If this is not baffled properly, either by the telescope optics or the infrared instrument, the contribution to infrared background radiation can be significant.

Wavelength Coverage

The likely wavelengths of interest in the thermal infrared ($>2 \mu\text{m}$) include the atmospheric windows at 2-2.4, 3-4.1, 4.5-5.1, 8-14, and 18-25 microns. Of these, the 2-2.4, 3-4, and the 8-13 micron window are typically clean enough that telescope emissivity becomes the dominant

source of noise. Figure 6-6 shows the expected sky background for dry conditions (1 mm PWV) and a 5% emissive telescope for comparison.

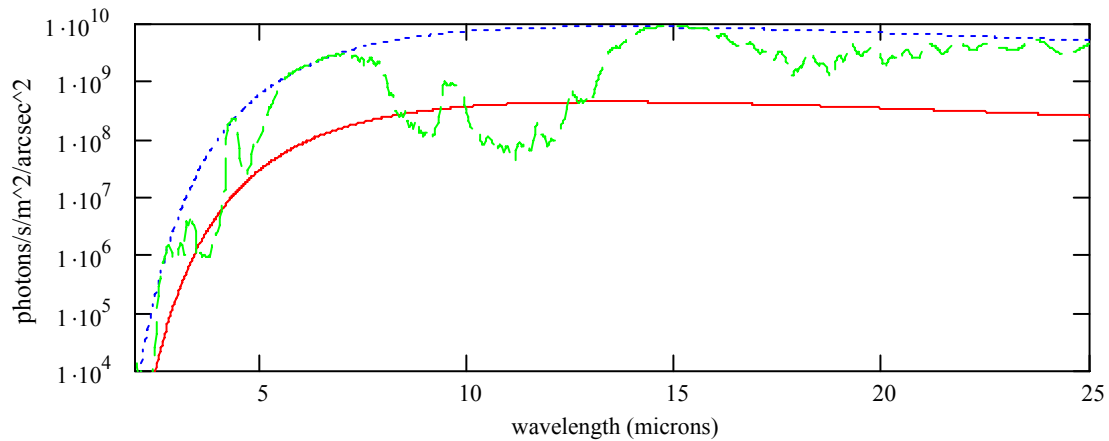


Figure 6-6. Modeled sky brightness for Mauna Kea from Gillette and Mountain 1998. The red line is the telescope background for a 5% emissive system.

Coating Contribution

For a well baffled optical system, the infrared background of the telescope will depend primarily on the coatings and cleanliness of the primary and secondary optics.

The standard coating for most telescopes is vacuum-deposited aluminum. This has the advantage of being a relatively robust coating with uniformly good reflectivity from the UV to the mid-infrared. Freshly deposited aluminum has reflectivity ranging from 96.8% -98% in the 2-10 μm wavelength range. Thus for two aluminized surfaces the expected emissivity of the system is 4-6.5% in this region.

The MMT, with an aluminum coated primary and secondary has a measured emissivity of approximately 7% at 10 microns. Emissivity measurements with the IRTF show similar levels (Toomey 1994). This increase over the nominal emissivity value is due at least partially to contamination which can be removed with periodic CO_2 cleaning. However degradation of the coating over time requires periodic recoating.

An alternative coating approach has been pioneered by Gemini to improve the infrared emissivity. A four layer silver coating has proven to be durable and resulted in emissivities as low as 2% for Gemini South (Boccas 2004). This approach may be a promising alternative for the GMT, with the potential drawback of decreased or lost blue sensitivity.

Background Radiation from Diffraction

Typical infrared-optimized telescopes have an optical design where the secondary forms the stop of the system (or is “undersized” compared to the primary mirror), creating an effective baffle for radiation from the warm telescope structure which would otherwise need to be baffled in the

instrument. Typical undersized secondaries such as the MMT and LBT f/15 secondaries are sized to be 98% of the critical diameter needed to match the primary. This creates an effective aperture for the telescope of ~96% of the collecting area. At a 12 arcminute field radius, vignetting by an undersized secondary for the GMT would produce an effective throughput of 92%.

In order to estimate the appropriate undersizing parameter for the GMT we can calculate the relative backgrounds of differently sized secondaries. The main contributor of background radiation is the warm structure just outside the edge of the primary mirror. If radiation from this material has either a direct or diffracted optical path to the focal plane, it will add unwanted background. It is straightforward to carry out a diffraction calculation which estimates what fraction of the warm telescope emission is diffracted into the beam, and we have done so using the approach sketched in Figure 6-7.

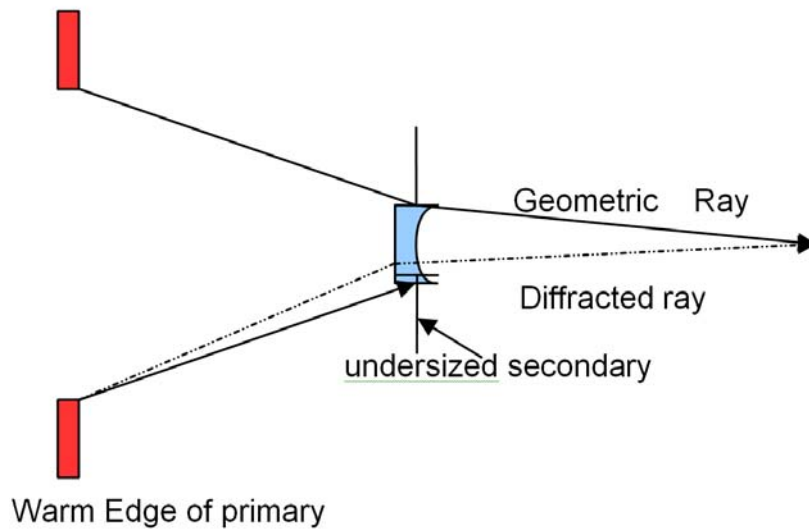


Figure 6-7. Setup for diffracted background contribution from warm material around the primary. If we model the secondary mirror as a lens which bends light through a geometrical angle, the rays from outside the primary reach the focal plane only if the secondary is oversized. If we undersize the secondary, light from outside the edge of the primary can only reach the focal plane through diffraction.

This calculation is carried out in two steps. The first step calculates the fraction of light diffracted into the beam by the secondary edge, taking into account the spread of the rays as they pass the secondary edge. To visualize this we can create an image of the secondary which shows how the diffracted light is distributed over the mirror. The calculation is carried out by tracing backwards rays from the focal plane. For an oversized secondary the edge of the primary is seen directly. For an undersized secondary a fraction of the light from the outer edge is bent into the beam. This is calculated by using a Gaussian probability for the rays to be bent a through non-zero angle for a given distance from the edge of the secondary.

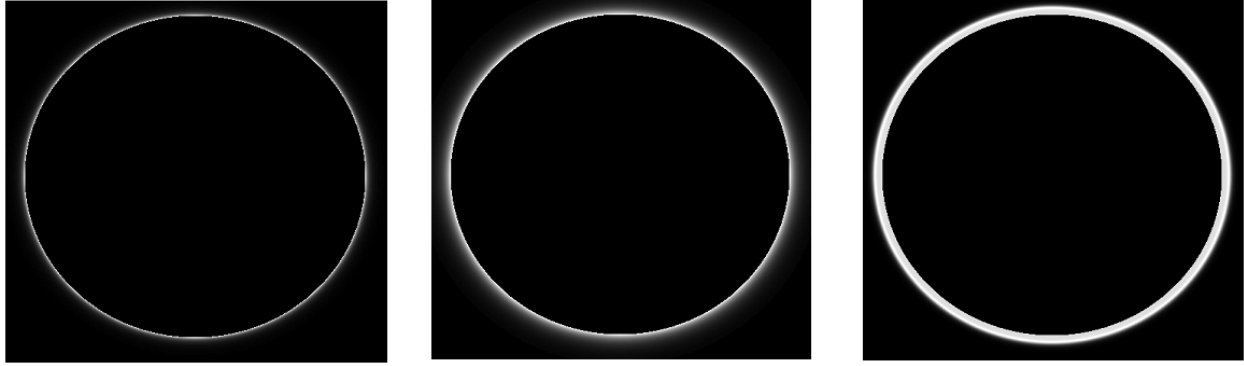


Figure 6-8. Distribution of light from the warm edge of the primary for three secondaries with 98%, 100%, and 105% of the primary diameter. Note the gray scale is not the same for each. The total emissivity in the beam would be 0.5%, 2.8%, and 13% respectively for the three cases.

To account for how much of this light actually makes it to the camera focal plane, we carry out a convolution of the secondary image in Figure 6-8 with an Airy pattern scaled to the resolution of a generic infrared camera. The only critical parameter of the IR camera is the size of its field stop, which determines the scale of the Airy pattern. We assume two different sizes: a 30" and a 1 arcminute circular field stop. The resulting images are masked with a cold stop which is scaled for 98% of the primary diameter. This whole calculation, illustrated in Figure 6-9, is only carried out for one 8.4 m GMT segment, but is approximately correct for the full GMT aperture.

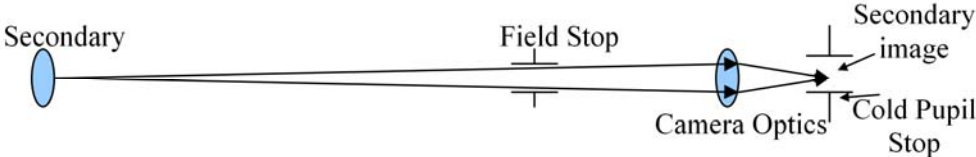


Figure 6-9. Reimaging the secondary onto a cold stop. The sharpness of the image is limited by the field stop.

To estimate the diffraction effect where it is most prominent we carry out the calculation at the longest wavelength where telescope background is likely to dominate: 13 μm . Results are shown in Table 6-2.

Table 6-2. Emissivity estimates calculated for various secondaries. Sizes listed are scaled to the fraction of the primary diameter it corresponds to.

Field size	Secondary Size (fraction)	0.98	1	1.05	1.1
30"		0.08%	0.3%	1.2%	1.4%
1'		0.04%	0.15%	0.6%	0.7%

For telescope emission dominated background regimes, Table 6-2 illustrates that there is little benefit to undersizing the secondaries. For secondaries matched to the size of the primaries (1 in the table above) the contribution to the emissivity is only 0.15-0.3%. This is in comparison to a

3-7% contribution from the mirror coatings. In the optimistic case (3% from mirror reflections), such a set up might increase the observing time needed by ~5-10% .

The above analysis assumes that the camera imaging of the secondary is only limited by diffraction. Optical aberrations will also spread the light out, increasing light from the outer edge. In effect, having a sky baffled secondary lessens the requirement on pupil imaging sharpness for infrared cameras on the GMT.

Flexure may also increase background emission for an oversized secondary if the camera does not have sufficiently stiff optics or mechanical interface to the telescope. Again, this may be resolved either by constraints on the camera, or by having the secondary sky baffled.

While undersizing the secondary will lessen the constraints on the infrared instrument imaging, the above calculations suggest that the amount of undersizing can be relatively small. Thus the baseline approach is to size the secondaries to be the critical diameter needed to match the primaries at zero field size.

6.3 Wide-field Corrector/Atmospheric Dispersion Compensator

6.3.1 Design Considerations

The uncorrected field aberrations shown in Figure 6-1 are growing with the square of the field size, and become objectionably large for field diameters larger than ~10 arcmin. The GMT baseline design is compatible with a wide-field corrector and atmospheric dispersion compensator to enable seeing-limited observations over fields larger than 10 arcmin at optical wavelengths. The instrument concept for the GMT wide-field optical spectrograph (GMACS, see Chapter 13) is based on the corrector/ADC, and in fact the optical designs of the secondary mirror, the corrector and the spectrograph collimators are the result of a single integrated conceptual development.

The current concept for the wide-field NIR spectrograph does not extend to field diameters larger than 10 arcmin, and the increased emissivity which would result from the use of a corrector/ADC in the NIR is a more serious limitation on performance than the relatively small transmission losses encountered in the optical. Because the optical materials, the coatings, and the design optimization of the corrector/ADC would all be seriously compromised in an attempt to produce a single unit working from the UV to the K band, the design of the corrector/ADC has not been extended to the near-infrared. A corrector design for the NIR is possible in principle, but would best be implemented as a separate unit.

A number of designs for field correctors have been considered as part of the GMT design process. Single plate aspheric correctors (Gascoigne 1965) do not provide adequate performance, but two-element spherical correctors produce images of very high quality. A third type of corrector adds a strong field lens near the focal plane to the two element design, in order to place the exit pupil at the center of curvature of a partially-flattened focal surface. We call this three-element design a telecentric corrector although in fact the term is a misnomer – for this design the chief ray is approximately perpendicular to the focal surface at all field positions.

The telecentric corrector has two advantages. (1) In order to implement a wide-field imaging spectrograph using a fly's-eye design, it allows an axially symmetric unit spectrograph to be optimized on-axis and then moved to an off-axis field location by rotating around the center of curvature of the focal plane. (2) In order to implement a wide-field fiber spectrograph, it allows a uniform set of buttons for a magnetically-positioned fiber system to be placed perpendicular to a plate which matches the radius of curvature of the corrected focal plane, without additional adjustment of the focus or angle of individual fibers.

The three-element telecentric corrector is the current baseline design for GMT. All three elements of the telecentric design must be optimized together, so it is not possible to produce a two-element corrector simply by removing the field lens from the optical path. Note that the choice of secondary mirror focal ratio is determined mostly by the optimization of the collimators for the optical and infrared wide-field spectrographs. The collimator designs for the uncorrected field, for use with a two-element corrector, and for use with the telecentric corrector are essentially similar. The main difference is that for the uncorrected or two-element cases, the field lens is placed after the telescope focal plane and is the first element of the collimator, while for the telecentric case, the field lens is placed in front of the telescope focal plane and is the last element of the corrector. The constraint on the secondary focal ratio arises mainly from the choice of the collimated beam diameter, and the baseline parameters for the secondary mirror are appropriate for nearly the same collimated beam diameter (300 mm) in all three cases.

The optical performance of the telecentric corrector does not depend strongly on the position of the leading element, as long as it is sufficiently far from the focal plane. Once the position of the leading element has been chosen, the position of the second element is a required degree of freedom in order to obtain good image quality. It turns out that for a particular position of the leading element, the first and second elements have net positive and negative power but very little bending into a meniscus shape. This case turns out to be mechanically convenient in terms of the deployment of the corrector behind the central mirror segment, as well as optically convenient for two reasons: (1) the volume of the glass blanks is minimized and slumping the blanks to a meniscus shape can be avoided, and (2) it is fairly convenient to split the second element into two pieces which incorporate rotating, zero-deviation prisms in order to implement an atmospheric dispersion compensator. This is the configuration which has been chosen as the baseline design for GMT and which is shown in Figure 6-10.

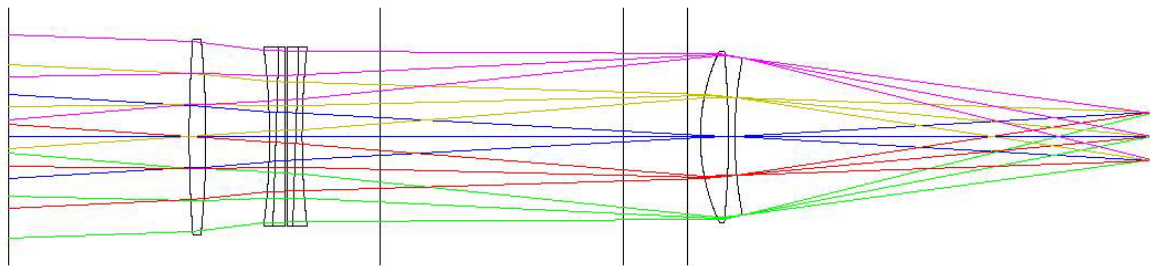


Figure 6-10. Optical layout of the GMT corrector/ADC. There are four mechanical reference planes shown in the diagram. At the left is the primary mirror vertex. Following the leading element of the corrector and the two rotating prisms is the bottom of the central mirror cell. The top and bottom of the instrument platform are shown immediately in front of the strong positive field lens. The curved focal plane is shown immediately following the field lens, and the exit pupil is shown at the right.

There are four reference planes shown in the diagram. From the left they are the position of the primary mirror vertex, the bottom of the center segment mirror cell, and the top and bottom surfaces of the instrument platform. The leading element and the two achromatic prisms are located inside the nominal volume of the center mirror cell. The field lens is located just below the instrument platform. The exit pupil is shown at the right of the diagram. The prisms are shown rotated so their dispersions cancel. The diameter of the leading element is 1.53 m.

A side view of the GMT corrector/ADC, in relation to the central mirror and mirror cell as well as the instrument platform, is shown in Figure 6-11. The corrector elements are shown in two positions inside the mirror cell: inserted along the optical axis in green, and retracted from the optical path in red. Adequate space is available for installation of the mirror support actuators between the bottom of the central mirror and the top of the retracted corrector.

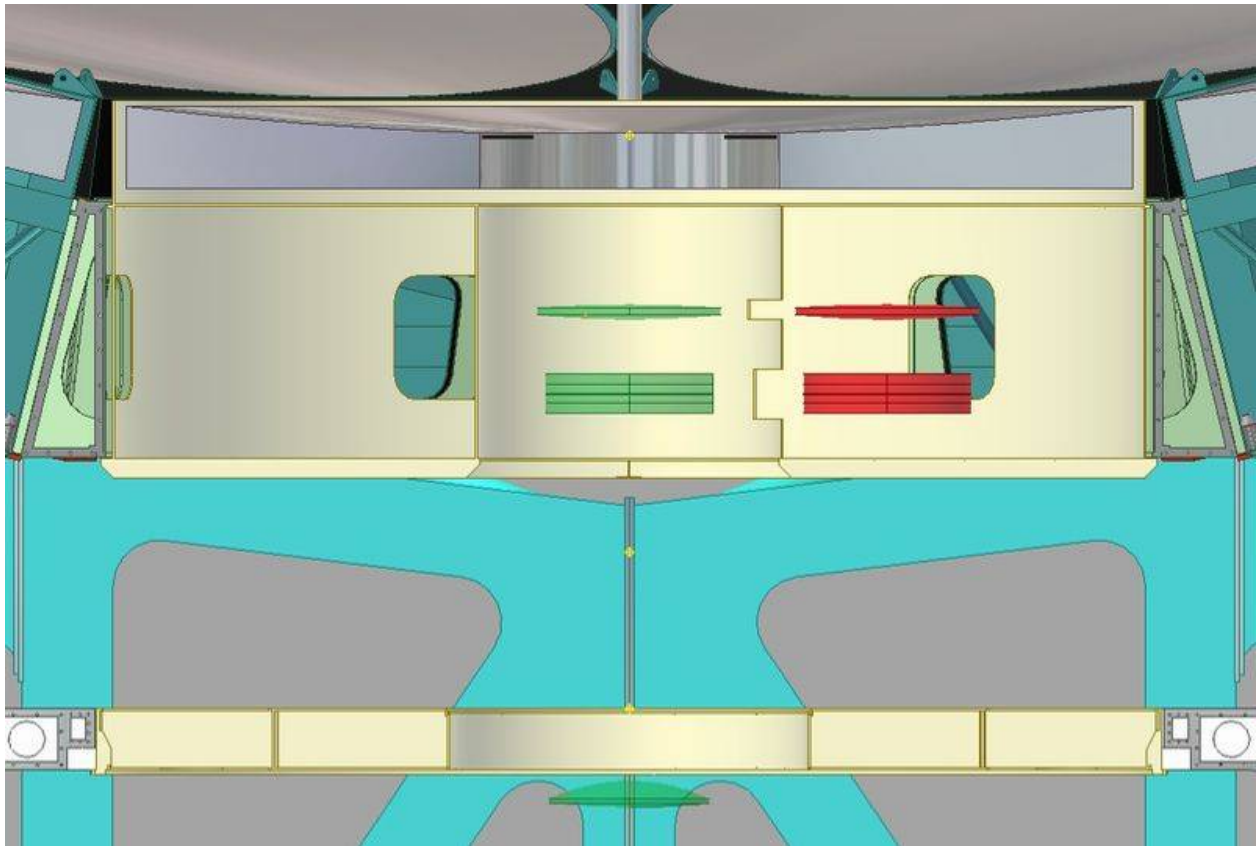


Figure 6-11. Side view of the GMT corrector/ADC, central mirror and mirror cell, and instrument platform. The corrector is shown inserted along the optical axis (*green*) and retracted from the optical path (*red*).

6.3.2 Optical Materials

The choice of optical materials for the GMT corrector/ADC is to some extent arbitrary. The “flint” elements of the zero-deviation prisms are typically made of LLF6 glass, which provides a reasonable amount of dispersion while maintaining good UV transmission, and can readily be made in the large sizes required (Jedamzik and Hartmann 2004). The “crown” elements of the prisms, and the leading element of the corrector, should all be made from the same glass in order

to avoid introducing chromatic aberration. The obvious choices for the crown elements are fused silica, FK5 and BK7. The field lens should also be made from one of these crown glasses, but it does not have to be the same as the one chosen for the leading elements.

Fused silica has the highest UV transmission and the best optical homogeneity, but the CTE mismatch with LLF6 means that the crown and flint elements of the prisms cannot be bonded together. BK7 and FK5 are better thermal matches which would allow the prisms to be bonded, perhaps with a compliant cement like Sylgard 184 RTV. While the UV transmission of FK5 is excellent, it is not clear whether this material can be obtained in the required sizes for the GMT corrector. Fused silica and BK7 should be available, although the field lens may be somewhat thicker than the nominal boule thickness for Corning fused silica.

Table 6-3 Properties of Corrector/ADC glasses

Glass type: Ohara I-line (Schott)	Fused Silica	FSL5Y (FK5)	BSL7Y (BK7)	PBL6Y (LLF6)
Transmission at 3500Å, 25 mm	1.	0.995 (0.988)	0.979 (0.93)	0.986 (0.93)
CTE, ppm/C	0.55	9.0 (9.2)	6.8 (7.1)	8.3 (7.5)

The baseline design for GMT adopts BK7 for the crown glass and LLF6 for the flint glass, except for the field lens which is fused silica. The total thickness of BK7 in the baseline design is 230 mm, and the total thickness of LLF6 is 140 mm. Clearly the Ohara I-line equivalents, or specially processed Schott glass for enhanced UV transmission, would be preferable. However since the transmission of all materials increases dramatically between 3500Å and 3800Å, it is clear that the corrector will begin to perform acceptably somewhere in this range of wavelength. The choice among the three crown glasses or their variants makes no difference to the corrected image quality, or to the optical design of subsequent elements such as collimators. The actual choice of glass will be left to a later phase of the design and will involve a detailed trade-off between availability, cost, UV transmission and CTE.

Finally, the trailing surface of the strong field lens needs to be aspheric. This improves the image quality of the exit pupil (or alternatively maintains the chief ray more nearly perpendicular to a spherical focal surface), without sacrificing other components of the merit function, in particular image quality in the focal plane. The maximum deviation from the best-fitting sphere is 1.87 mm (the total sag is 32 mm), but since this surface is very close to the focal plane, the required optical precision is relatively low. It should be possible to obtain adequate metrology for this surface during polishing by using a relatively simple profilometer like the one that was used for the Sloan aspheric field flattener (Ed Mannery, private communication).

6.3.3 Performance

The two-element correctors can produce extremely good images over any practicable field size. However the performance of the three-element telecentric design tends to degrade for very large

fields, and the volume of the field lens becomes extremely large. For these reasons the field of view of the GMT baseline corrector has been limited to 20 arcmin.

The spot diagram for the corrector/ADC pointing at the zenith is shown in Figure 6-12. Even though the design is slightly non-axisymmetric because of the introduction of the prisms, the images are almost identical at a given field radius. The rms polychromatic spot diameter increases from 0.03 arcsec at the center of the field to 0.07 arcsec at the edge of the field. For comparison, the uncorrected rms image diameter at the edge of a 20 arcmin field would be 0.62 arcsec.

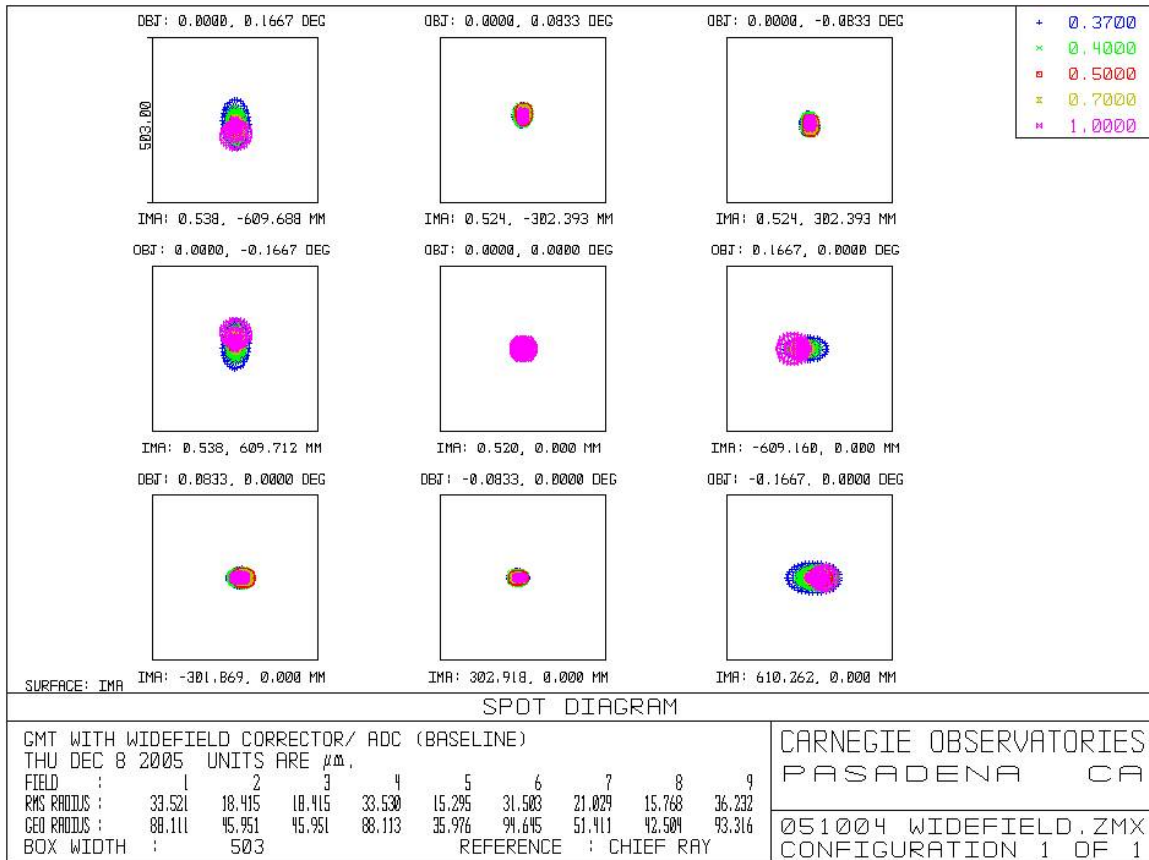


Figure 6-12. Polychromatic spot diagram for the baseline GMT corrector working at the zenith. The box size is 0.50 arcsec.

The prism angles in the ADC are selected in order to compensate for atmospheric dispersion up to a specified zenith angle. As the prisms become stronger the optical performance at the zenith degrades slightly, and the elements become larger and more difficult to fabricate. The prisms in the GMT baseline corrector have been specified to fully compensate for atmospheric dispersion up to a zenith angle of 50°. As the telescope moves away from the zenith the prisms are rotated with respect to each other, from the fully-cancelled position at the zenith to the fully-additive position at a zenith angle of 50°. The resulting spot diagram is shown in Figure 6-13.

At an altitude of 2400 m, the uncorrected atmospheric dispersion (0.37-1.00 μm) at a zenith angle of 50° forms a spectrum which is 1.98 arcsec long. The ADC fully cancels the linear dispersion, but there is a residual quadratic term because the dispersion curve of the two glasses does not exactly match that of the atmosphere. The residual quadratic spectrum (0.37-1.00 μm) is 0.17 arcsec long. The symmetry of the correction of field aberrations in the blue is disturbed slightly by rotating the prisms, but the effect is small compared to the quadratic spectrum. In principle the exact rotation setting of the prisms can be adjusted for smaller bandpasses, in which case the length of the residual spectrum will decrease approximately with the square of the bandpass.

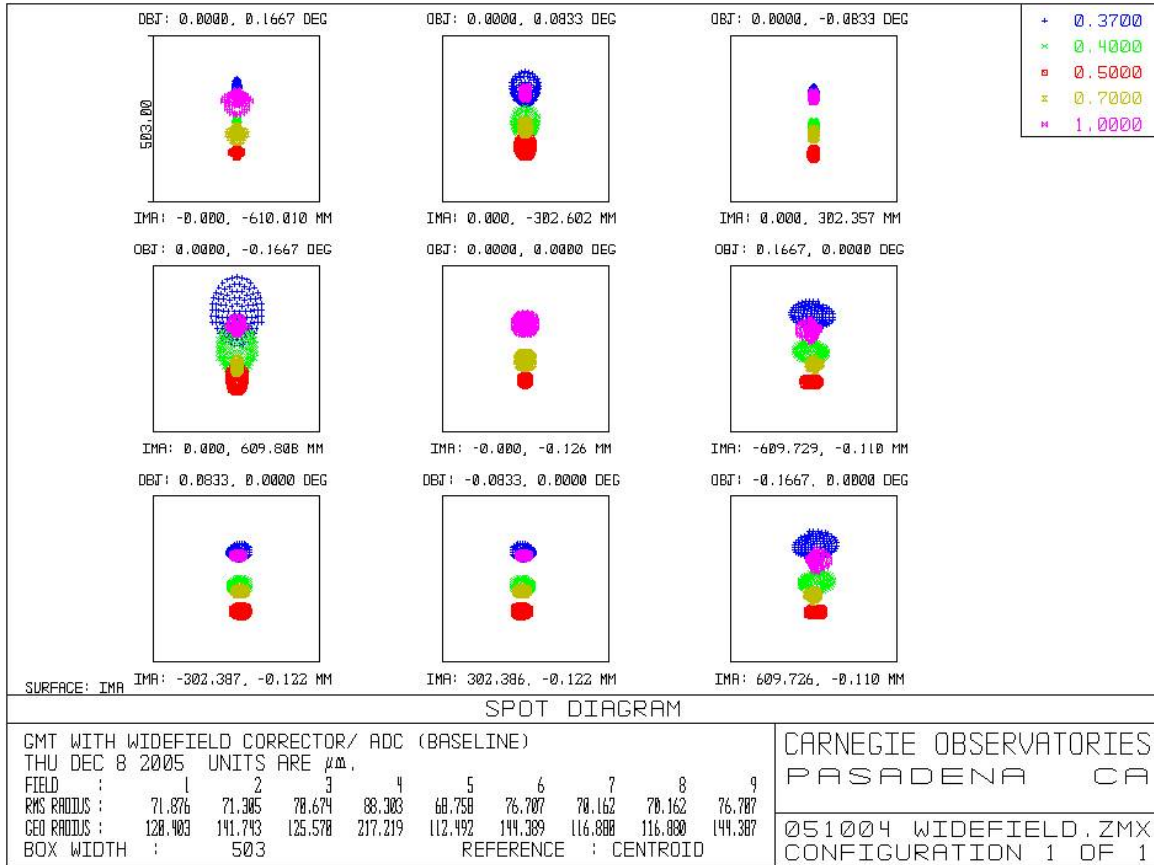


Figure 6-13. Polychromatic spot diagram for the baseline GMT corrector working at a zenith distance of 50° . The box size is 0.50".

6.3.4 Alignment

The telecentric corrector/ADC will presumably be implemented in two modules. The first module will be part of the central mirror cell and will allow the leading element of the corrector and the prisms to be inserted into the optical path (or removed) as a unit. The second module will contain the field lens and will be part of the focal plane assembly of the wide-field spectrograph, which will also contain the slit mask (or fiber plate), guiders and image analyzers. The focal plane assembly will be located below the instrument platform. Pending further

elaboration of the mechanical design, it seems reasonable to suppose that the accurate alignment of the components within each of these modules (e.g. the alignment of the leading element with respect to the prisms, or the alignment of the field lens with respect to the slit mask) will be relatively easy to achieve and to maintain. The more interesting question is how accurately the two modules must be aligned relative to each other and relative to the optical axis of the telescope.

The effects of two lateral displacements have been investigated: (1) the lateral alignment of the whole corrector and focal plane assembly with respect to the optical axis defined by the primary and secondary mirrors, and (2) the lateral alignment of the focal plane assembly (including the field lens) with respect to everything in front. There are two quantities to track as the lateral misalignment is increased: (1) image quality, and (2) deviation from the “telecentric angle” as a function of field position. The tolerance for image quality will be specified as part of the overall image error budget. The tolerance for the telecentric angle will be set by the acceptable level of light loss caused by misalignment of the exit pupil with respect to the collimator optics. The half-angle of an f/8 cone is 3.6 deg. For a fiber system the ray azimuths are scrambled, so an error in the telecentric angle of 0.1 deg will result in an exit cone with a half-angle of 3.7 deg, and a loss of efficiency of about $[1 - (3.6/3.7)^2] = 5\%$. For an imaging spectrograph a 0.1 deg error in the telecentric angle will deflect the exit cone by 0.1 deg, resulting in a loss of efficiency of about $[0.1/7.2] = 1.4\%$.

For the case of a displacement at the entrance to the corrector, the results are summarized in the following table:

	rms spot dia, polychromatic				telecentric angle, deg			
	0	10	14.1	20	0	10	14.1	20
Field dia:	0	10	14.1	20	0	10	14.1	20
Displ	-----	-----	-----	-----	-----	-----	-----	-----
-20 mm	0.052	0.254	0.379	0.493	0.043	0.040	0.026	0.046
-10 mm	0.047	0.139	0.209	0.243	0.021	0.017	0.004	0.031
-5 mm	0.046	0.080	0.123	0.120	0.011	0.006	0.007	0.024
0 mm	0.045	0.028	0.038	0.049	0.000	0.006	0.018	0.017
5 mm	0.046	0.050	0.058	0.156	0.011	0.017	0.029	0.010
10 mm	0.047	0.110	0.146	0.285	0.021	0.028	0.040	0.004
20 mm	0.052	0.237	0.330	0.469	0.043	0.051	0.062	0.008

Note that these calculations were performed on an earlier optimization of the corrector than the one shown in Figure 6-10. For the earlier optimization, the image size is slightly worse at the center of the field and slightly better at the edge of the field. The displacements in the table are very large in order to emphasize the trend in image size with lateral displacement. The rms polychromatic image diameter degrades at the rate of 0.025 arcsec per mm (in quadrature with the spot size at zero displacement). This is the worst value at the edge of the field. An acceptable displacement is likely to be in the range of about 1 mm. A 5 mm displacement would be noticeable in very good seeing. The error in the telecentric angle is much smaller than 0.1 deg for any plausible displacement.

For the case of a displacement of the focal plane assembly including the field lens, the results are:

Field dia:	rms spot dia, polychromatic				telecentric angle, deg			
	0	10	14.1	20	0	10	14.1	20
Displ	-----	-----	-----	-----	-----	-----	-----	-----
-20 mm	0.066	0.261	0.385	0.500	0.089	0.086	0.073	0.093
-10 mm	0.051	0.143	0.212	0.246	0.045	0.040	0.027	0.055
-5 mm	0.047	0.083	0.124	0.121	0.022	0.017	0.004	0.036
0 mm	0.045	0.028	0.039	0.049	0.000	0.006	0.018	0.017
5 mm	0.047	0.050	0.061	0.159	0.022	0.028	0.041	0.001
10 mm	0.051	0.112	0.150	0.288	0.045	0.051	0.063	0.019
20 mm	0.066	0.242	0.336	0.488	0.089	0.097	0.108	0.055

In this case the image quality degrades at almost exactly the same rate as for a displacement in front of the corrector. The telecentric angle degrades about twice as fast, but is still small for any plausible displacement.

6.3.5 Manufacturing Considerations

A bill of materials for the corrector/ADC is instructive:

#	Glass	Dia	Max thk	cyl/net kg
--	-----	-----	-----	-----
1	BK7	1530	130	631/446
2	BK7	1400	114	497/275
3	LLF6	1400	93	464/303
4	LLF6	1400	93	464/303
5	BK7	1400	114	497/262
6	SILICA	1340	220	709/403

The sizes of the elements are given in mm. The weights given in the last column are for cylindrical blanks and for finished elements. It is possible that elements 2 and 5 (the crown prismatic lenses), and elements 3 and 4 (the flint prisms) could be cut at an angle from single blanks which would be thicker than the individual blanks shown in the table but thinner than both blanks added together.

If they are bonded together, the achromatic prisms in the GMT corrector would be similar to the corrector/ADC elements in Magellan, although considerably larger in diameter (1400 mm vs. 740 mm). Bonding the Magellan prisms was a problem because the individual elements were too thin to maintain their figure during the bonding process. The result was that the glue layer exhibited measurable variations in optical path length on scales comparable to the diameter of the pupil as it propagates through the corrector. Post-polishing of the bonded elements was required in order to correct these errors, which interfered with the plan for AR coating the corrector elements prior to bonding.

The diameter of the pupil where it is propagating through the GMT prisms is 380 mm, about the same as it is for the Magellan field corrector. However in the GMT design, the thinnest dimension of each prism element has been increased to 50 mm, compared to only 16 mm in Magellan. For this reason the GMT elements will be dramatically stiffer on the scale of the pupil diameter. Moreover in the seeing-limited case, the larger scale of the GMT focal plane (or equivalently of the entrance aperture) will lead to a relaxed specification on the allowable wavefront error on the scale of the pupil, as compared to Magellan. Further analysis should confirm that the GMT prisms are stiff enough to be bonded without requiring post-polishing, and optimization of the thickness might result in a moderate improvement in UV transmission over the current design.

6.4 Optical Coatings

Aluminum is the simplest broadband film to deposit and it will be the starting point for developing hybrid high reflectivity coatings. Recent applications of multiple layer coatings on large telescope optics make high performance long life films possible for 8.4 meter mirrors.

Gemini and VLT have developed coating systems using linear magnetron sputtering sources on large diameter mirrors. Gemini is using a protected silver formula on all of their mirrors. The layers are chromium, silver, chromium, and silicon nitride. These are deposited in different thickness to obtain the desired results. The Gemini chamber has three different linear magnetron sources, one for each material, on a common mount and uses rotation of the mirror and radial motion of the head to deposit the coating. While there were early failures in the first coatings the latest version has been in use for 18 months and has performed up to expectations. Figure 6-14 shows typical reflectance curves for aluminum and the new Gemini 4 layer protected silver coating. Note the strong decrease in reflectance as the coating approaches 400 nanometers. GMT will coat its primary mirror segments with traditional aluminum to maintain high throughput in the near UV but will investigate other possibilities in the next phase.

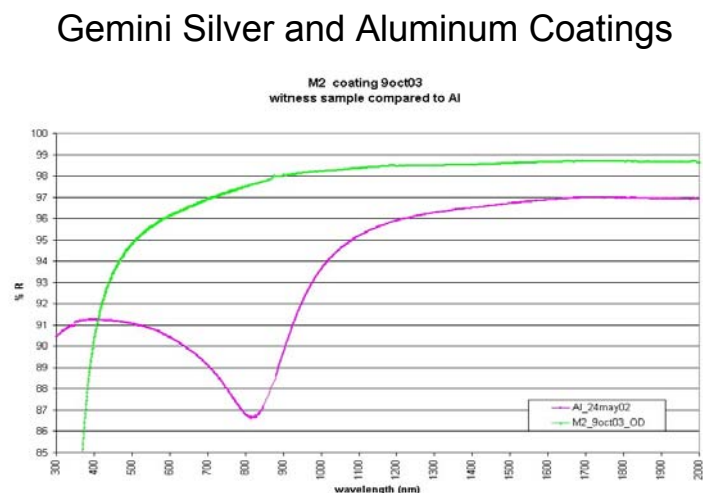


Figure 6-14. Gemini coating curve. Reflectivity of silver and aluminum coatings from 300 nm to 1.2 μm .

VLT has been depositing sputtered aluminum on their mirrors for over five years with very good results. VLT also uses a radial scan system to deposit the coating. GMT will most likely use a linear scan to avoid coating overlap at the center of the off-axis mirrors which have no large central hole.

These two large diameter coating systems show that sputter deposition is a viable means of coating large mirrors and that is what has been selected as the baseline for GMT. Sputtering deposition allows a wide selection of materials to be deposited with the same hardware. The primary mirror coating system is described in Chapter 15.

6.5 Technical Challenges and Risks

The fast optical design reduces the overall size of the telescope structure and elements in the optical train (secondary mirror, correctors, etc.) but requires highly aspheric off-axis optics and close alignment tolerances. These are challenging but the project believes they are achievable based on feasibility studies carried out to date and the experience with the current generation of large borosilicate mirror telescopes and work underway to demonstrate these capabilities. Developing the metrology for in-process testing during fabrication and the metrology for maintaining alignment and phasing during operation in the telescope will be key objectives of the design development phase.

The focal lengths of the seven individual sub-apertures are required to match to high precision. This places stringent tolerances for the radii of curvature of the primary and secondary mirror segments. Some relaxation of the tolerances required for mirror fabrication will be possible allowing for active correction of the mirror figure in the telescope. These issues will be discussed in Chapters 10 and 11 dealing with the primary and secondary mirror requirements.

The large fused silica and glass elements for the wide-field corrector and atmospheric dispersion compensator push and for the most part exceed sizes of high quality refractive material currently available from commercial vendors. The fast optical design of the GMT minimizes the diameters but a development effort in collaboration with suppliers will be required to obtain these elements. Discussions with glass manufacturers are already in progress. The glasses in the corrector and ADC design were selected with this issue in mind. In some cases alternate glasses are available with some trade-off in performance.

6.6 REFERENCES

Chaffee, F. H., et al. 1990, in SPIE Conf. Ser. 1236, Advanced Technology Optical Telescopes IV, ed. Lawrence D. Barr (Bellingham: SPIE), 507

Gascoigne, S. C. B. 1965, Observatory 85, 79

Hill, J., Salinari, P. 2004, in SPIE Conf. Ser. 5489, Ground-based telescopes, ed. J. M. Oschmann, Jr. (Bellingham: SPIE), 42

Jedamzik, R. and Hartmann, P. 2004, in SPIE Conf. Ser. 5494, Optical Fabrication, Metrology and Material Advancements for Telescopes, ed. E. Atad-Ettinger and P. Dierickx (Bellingham: SPIE), 382

Shectman, S. 2000, in SPIE Conf. Ser. 4004, Telescope structures, enclosures, controls, assembly/integration/validation, and commissioning, ed. T. Sebring, T. Andersen (Bellingham: SPIE), 47

West, S. C., et. al. 1996, in SPIE Conf. Ser. 2871, Optical telescopes of today and tomorrow: following in the direction of Tycho Brahe, ed. A. Ardeberg (Bellingham: SPIE), 38